Journal of Power Sources 214 (2012) 59–67

Contents lists available at SciVerse ScienceDirect

Journal of Power Sources

journal homepage: www.elsevier.com/locate/jpowsour

# Effect of mechanical vibration on platinum particle agglomeration and growth in Polymer Electrolyte Membrane Fuel Cell catalyst layers

Georgiy Diloyan [a], Marcus Sobel [b], Kiranmoy Das [b], Parsaoran Hutapea [a,*]

[a] Department of Mechanical Engineering, Temple University, 1947 N 12th Street, Philadelphia, PA 19122, USA
[b] Department of Statistics, Temple University, 1947 N 12th Street, Philadelphia, PA 19122, USA

## HIGHLIGHTS

- The effect of mechanical vibration on Pt particle growth in PEMFC was investigated.
- Transmission electron microscope and statistical regression model were utilized for the study.
- Mechanical vibration caused a decrease in Pt particle growth rate in the catalyst layers.

## ARTICLE INFO

*Article history:*
Received 30 January 2012
Received in revised form
12 April 2012
Accepted 16 April 2012
Available online 27 April 2012

*Keywords:*
PEM Fuel Cells
Vibration
Platinum growth
Catalyst layer
Accelerated test

## ABSTRACT

The effect of mechanical vibration on Platinum (Pt) particle agglomeration and growth in the catalyst layer of a Membrane Electrode Assembly (MEA) for a Proton Exchange Membrane Fuel Cell (PEMFC) was investigated. A series of experiments were conducted using a 300-h accelerated test with potential cycling and transmission electron microscopy (TEM). Each of the 300-h accelerated tests used different constant mechanical vibration conditions (frequency and acceleration). It was observed that the average diameter of Pt particles under vibration is 10% smaller than the ones that were under no vibration conditions. The Pt particles in the order of 2–2.5 nm in the pristine state have grown to approximately 6 nm (after 300-h accelerated test without vibration condition) and to approximately 5.47 nm (after 300 h accelerated test under 1 g 20 Hz vibration condition).



## 1. Introduction

Polymer Electrolyte Membrane Fuel Cell (PEMFC) has been the focus of many studies as an alternative to Internal Combustion Engines (ICE) because of their zero-emissions and high efficiency [1–4]. Although PEMFC has been considered to be one of the most attractive candidates for automotive applications, its components, including carbon-supported platinum catalyst, have yet to meet requirements such as durability and the mass activity of the Oxygen Reduction Reaction (ORR) [5–11].

Carbon-supported platinum as a catalyst material has very high kinetics for the Hydrogen Oxidation Reaction (HOR). Comparing to the HOR reaction, kinetics of the platinum for ORR is slow. However, platinum remains the most preferable catalytic material. It has one of the best electrode performances at low temperature and acidic environment inside PEMFC. In recent years, scientific experiments have been conducted to study carbon-supported platinum and its stability, including its agglomeration and growth [11–22]. The catalyst stability depends on several factors such as potential, temperature, humidity, and contamination. For example, Lin et al. [18] have studied the effect of dynamic loading cycling on the degradation and Pt growth. Rapid degradation of the performance was observed after 280 h of the fuel cell operation. Additionally, Pt growth was observed after 370 h of testing. For this experiment, fuel cell was not introduced to any mechanical loading, only to the voltage loading cycle for simulating driving conditions.

In addition to potential cycling, other influencing factors on Pt particle agglomeration and growth have been studied by many researchers. It has been well established that hydrogen influences the agglomeration and growth of Pt particles [17,23–26]. In a study by Darling and Meyers [23], they proposed a three-stage Pt growth model that includes Pt dissolution, formation of Pt ions, and removal of ions from the system by hydrogen that has crossed over Membrane Electrode Assembly (MEA) from the anode to the cathode. In the first stage, Pt oxides are forming under high

* Corresponding author. Tel.: +1 215 204 7805; fax: +1 215 204 4956.
*E-mail address:* hutapea@temple.edu (P. Hutapea).

0378-7753/$ – see front matter © 2012 Elsevier B.V. All rights reserved.
doi:10.1016/j.jpowsour.2012.04.027

potentials at the cathode side as explained in Eq. (1). In the second stage Pt oxide dissolution process occurs with formation of Pt ions as illustrated in Eq. (2). Finally, in the third stage, the Pt ionic species are removed from the system as described by Eq. (3), which is called the precipitation reaction. In this stage Pt ions are getting reduced to Pt particles by hydrogen crossed over the MEA from anode to cathode side.

$$Pt + H_2O \rightarrow PtO + 2H^+ + 2e^- \quad (1)$$

$$PtO + 2H^+ \rightarrow Pt^2 + H_2O \quad (2)$$

$$Pt^2 + H_2 \rightarrow Pt + 2H^+ \quad (3)$$

Chen et al. [24] studied the effect of hydrogen crossover on Pt agglomeration and growth. It was observed that local concentration of Pt ions was higher at the cathode catalyst layer when there was less crossover hydrogen and based on the observation it was hypothesized that hydrogen crossover chemically reduces Pt oxides and decreases the amount of Pt ions formed via the oxide pathway. This observation suggested that Pt growth would be higher in the case with less hydrogen crossover, since there was higher concentration of Pt ions available for deposition and crystallite growth.

Although Pt agglomeration and growth have been studied by many researchers [11–22], few have considered studying the effect of mechanical loadings such as the effect of vibration on the Pt agglomeration and growth. For PEMFC to be used as an alternative energy source in vehicular applications [1,4,27,28], the effect of mechanical loadings, such as due to vibration in automobiles, on the fuel cell performance and durability needs to be fully understood and studied. Through a literature survey, it is apparent that there is a lack of studies discussing the influence of vibration, especially for a long-term test procedure. A few studies, such as the one conducted by Rajalakshmi et al. [29], discussed the effects of shock and vibration for a short duration. In their study, the fuel cell stack was undergoing horizontal and vertical vibration with the amplitude of acceleration of 3 g and a frequency range of 30–150 Hz. The duration of the test was 90 min for each of the vibration cases. For studying a shock effect, acceleration was kept at 30 g for 10 pulses for 15 ms each. The performance of the fuel cell stack was recorded before and after the vibration and shock test. The results of the study showed that vibration does not affect the performance of the fuel cell stack. They have recommended further dynamic life testing.

In another study, Rouss and Charon [30] developed a model for the mechanical nonlinear behavior of a PEMFC system subjected to vibration. Raw experimental data was used to create a multi-input and multi-output (MIMO) model using a multi-layer perceptron neural network combined with a time regression input vector. Results from the analysis showed good prediction accuracy. In the study conducted by Bétournay et al. [31], the effects of underground mining conditions, gases, dust, shock and vibration on the performance of PEMFC were investigated during extensive testing in an operating underground metal mine. The fuel cell was tested during 50 h for different vibration test types and exposed to mine contaminant levels using air intake filters. After the tests, the *V–I* (Voltage–Current) curve did not show any significant damage, but further tests were recommended.

In our research, a study evaluating the effect of vibration on Pt particles agglomeration and growth and PEMFC performance was conducted. First, a 300-h accelerated test procedure with potential cycling and vibration conditions was designed to simulate real life long-term fuel cell operation. It should be mentioned again that the effect of potential cycling during accelerated tests on the Pt agglomeration and growth has been discussed by many researchers [16,32–36,39]; however, in their studies the effects of vibration have not been considered. Second, during the 300-h accelerated test, the PEMFC performance and operating parameters were monitored and controlled by a fuel cell test station. Experimental procedures using Transmission Electron Microscope (TEM) were conducted to quantify the Pt particle size. The Pt particle size of the MEA catalyst layer was observed after the end of each of the 300 h accelerated test. Lastly, a statistical method was used to interpret the observed data. The research method, results, and conclusions are presented in the following sections.

## 2. Experimental method

The accelerated degradation tests were performed using a fuel cell hardware assembly connected to a test station (Fuel Cell Technologies, Inc., New Mexico, USA) as shown in Fig. 1. The fuel cell hardware assembly has a 25-$cm^2$ active surface area. A N115 catalyst-coated MEA made by DuPont Fuel Cells (Delaware, USA) was used. The Pt loading for each of the N115 MEAs was 0.3 mg Pt $cm^{-2}$, both for the cathode and anode sides. The Sigracet 25 (SGL Carbon SE, Wiesbaden, Germany) for the gas diffusion layer (GDL) and PTFE-coated fiberglass fabric (Precision Coating Co., Inc., Massachusetts, USA) for the gaskets were used. The PEMFC was assembled by compressing MEA, GDL, and gaskets (from anode and cathode sides) between bipolar plates (BP) and end plates (EP). The endplates were tightened by screws at a torque of 13 Nm.

The experimental approach included the following steps: (i) run the accelerated test with potential cycling and under vibration conditions; (ii) monitor performance of the fuel cell during accelerated test using the fuel cell test station; and (iii) visualize and analyze Pt particle diameter size in the degraded MEA (after the accelerated tests) using Transmission Electron Microscope (TEM) (JEOL JEM-1400).

### 2.1. Accelerated test procedure

Based on reviewed articles and tests performed by different researchers [16,18,32–39], the accelerated test was designed to study Pt agglomeration and growth and PEMFC performance operating under vibration. This test was conducted to simulate the performance of a fuel cell under real driving conditions, where the effect of vibration is very common.

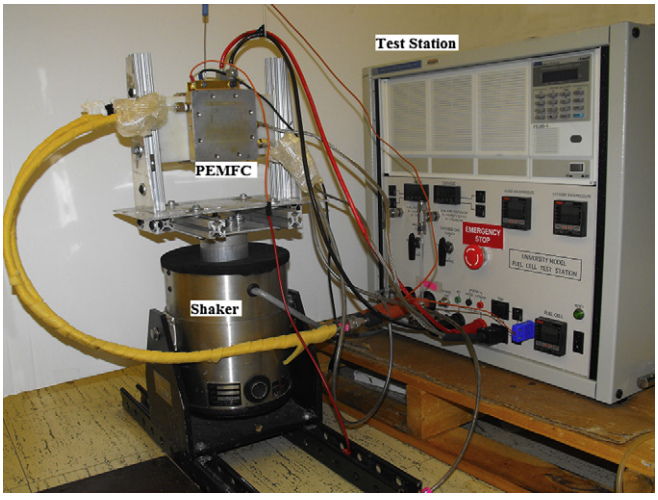


**Fig. 1.** Fuel cell test station with PEM Fuel Cell hardware installed on a VTS shaker.

To accelerate the catalyst layer degradation, each MEA was subjected to a 300-h potential cycling following the procedures described in the literature [18,29,37–39] and mechanical vibrations based on typical vibration conditions of moving vehicles [28,30]. The potential cycle and accelerated test conditions are shown in Tables 1 and 2. The accelerated test simulated idle running (OCV), constant load running, variable load acceleration, and overload running conditions.

As discussed by Lin et al. [18], the rapid performance drop was investigated after 280 h of fuel cell operation and Pt growth was observed after 370 h of testing. In the study of Garland et al. [34], the electrocatalyst was subjected to 500 h two-step potential cycling at 0.7 and 0.9 V with 30 s at each step. In order to apply more aggressive test conditions, such as vibration and rapid voltage change (triangle step voltage), the length of the accelerated test was designed to be 300 h. The parameters of the accelerated test are shown in Table 3. The vibration experiments were conducted using a shaker (Vibration Test Systems, Inc., Ohio, USA) (Fig. 1) with different parameters of oscillations: 20 Hz and 40 Hz (1 g and 4 g of magnitude). The vibration frequencies for the test were chosen to be close to real vehicle frequencies during its operation (17–40 Hz) [40]. The maximum magnitude of vibration of the vehicle usually does not exceed 0.95 g [30]. However, to apply more aggressive test conditions, the PEMFC was tested under the acceleration of 1 g and 4 g.

### 2.2. Pt particle measurements

To study the Pt agglomeration and growth on a catalyst layer of the fuel cell MEA, the Transmission Electron Microscopy (TEM) (JEOL JEM-1400) was utilized. TEM is a destructive microscopy technique where an electron beam is transmitted through a thin specimen. TEM was used to quantitatively measure platinum particle sizes on the cathode and the anode sides. The Pt particles from the MEA were removed by scraping catalyst layer with a scalpel and dissolving it in a pure ethanol. The solution was then sonicated for 1.5 h in order to separate the Pt particles from carbon support. After the sonication, 1 μL of solution was deposited on a TEM grid for imaging. Images from the TEM procedures were analyzed using ImageJ software [41]. The high concentration of the Pt particles on some images and the low contrast between the edges of the particles did not allow the use of the available automatic particle count procedure. Therefore, a manual approach was used. In this approach each distinct Pt particle on TEM images was selected, counted, and analyzed separately. The number of Pt particles counted was dependent on the number of available samples and TEM images and therefore varied from sample to sample. The total number of Pt particles counted during image analysis process for each case is listed in the sixth column of Tables 4 and 5. In our study, the performance and microscopy data was obtained from fourteen specimens tested at different vibration conditions and time durations. As shown in Table 3, the vibration test conditions are: 1 g 20 Hz (Case 1), 1 g 40 Hz (Case 2), 4 g 20 Hz (Case 3), 4 g 40 Hz (Case 4) and no vibration (Case 5). All vibration tests were repeated twice. In addition, different time duration tests were performed for the statistical Pt particle size prediction model. The tests with various time durations are: 2 h (T1), 50 h (T2), 126 h (T3), 300 h (T4 Case 5) and 420 h (T5). Please note that the length of the tests T3 and T5 ended up being 126 and 420 h due to equipment problems respectively.

**Table 1**
Potential cycle of the accelerated test.

| Potential cycle of the accelerated test | |
|---|---|
| Step | Description |
| OCV – 1 V | 20 s |
| Triangle step voltage, two way 095 V–0.45 V | 0.05 V/5 s |
| OCV – 1 V | 20 s |
| Constant load running –0.75 V | 60 s |
| Full power – 0.5 V | 40 s |
| OCV – 1 V | 20 s |
| Overload running, one way 0.5 V–0.4 V | 0.05 V/10 s |

**Table 2**
Accelerated test conditions.

| Accelerated test conditions | |
|---|---|
| Fuel/Oxidant | Hydrogen/Air |
| Fuel Cell temperature | 80 ± 1, °C |
| Backpressure | 4, psi |
| Hydrogen humidity | 100, % |
| Oxygen humidity | 100, % |
| Hydrogen temperature | 80 ± 1, °C |
| Oxygen temperature | 80 ± 1, °C |
| Hydrogen flow, stoic | 1.5 |
| Oxygen flow, stoic | 2.5 |
| Test length | 300, h |

## 3. Data analysis

To analyze the data collected after each 300-h accelerated test (Case 1–Case 5), a box plot diagram [42] was used. The box plot summarizes certain statistical measures, such as median (middle value – red line in the box), upper and lower quartiles, and minimum and maximum data values (lower and upper whisker). Outliers are marked in red above the upper whisker.

In order to elucidate the statistical significance of Pt particle sizes after the 300-h accelerated test under vibration conditions, an analysis of variance (ANOVA) [42] and multiple comparison [42] tests were conducted. An ANOVA test can be used to explain whether there are statistically significant differences somewhere in the data. But it cannot tell specifically where those differences are. For this reason a combination of ANOVA and multiple comparison tests was conducted to check a null hypothesis. The null hypothesis in this study was defined as follows: mean Pt particle sizes between each 300-h accelerated test under vibration conditions (Case 1–Case 5) are the same.

In addition, the collected data (Case 1–Case 5 and T1–T5) was used to develop a statistical model that describes the Pt particle growth as a function of time (t), frequency (Hz) and acceleration (g). At this moment the model predicts Pt particle size in the time range up to 300 h and in various vibration ranges up to 40 Hz and 4 g.

In order to insure that the model exemplifies only systemic and not noisy vibration condition effects, a regression model was

**Table 3**
Vibration test schedule.

| MEA # | Time, h | Acceleration, g | Frequency, Hz |
|---|---|---|---|
| Case 1 | 300 | 1 | 20 |
| Case 2 | 300 | 1 | 40 |
| Case 3 | 300 | 4 | 20 |
| Case 4 | 300 | 4 | 40 |
| Case 5–T4 | 300 | 0 | 0 |
| T1 | 2 | 0 | 0 |
| T2 | 50 | 0 | 0 |
| T3 | 126 | 0 | 0 |
| T5 | 420 | 4 | 20 |

**Table 4**
Pt particle sizes after various vibration condition tests.

| Test | Time, h | Acceleration, g | Frequency, Hz | Pt particle mean diameter, nm | Number of particles counted | Pt particle median diameter, nm |
|---|---|---|---|---|---|---|
| Case 1 | 300 | 1 | 20 | 5.55 ± 1.16 | 1348 | 5.47 |
| Case 2 | 300 | 1 | 40 | 5.89 ± 1.41 | 636 | 5.76 |
| Case 3 | 300 | 4 | 20 | 5.64 ± 1.42 | 1128 | 5.49 |
| Case 4 | 300 | 4 | 40 | 5.89 ± 1.21 | 876 | 5.8 |
| Case 5 | 300 | 0 | 0 | 6.14 ± 1.53 | 1505 | 6 |

**Table 5**
Pt particle sizes after various time duration tests.

| Test | Time, h | Acceleration, g | Frequency, Hz | Pt particle mean diameter, nm | Number of particles counted | Pt particle median diameter, nm |
|---|---|---|---|---|---|---|
| Pristine state | 0 | 0 | 0 | 2.34 ± 0.38 | 173 | 2.3 |
| T1 | 2 | 0 | 0 | 3.34 ± 0.55 | 155 | 3.34 |
| T2 | 50 | 0 | 0 | 4.48 ± 1.04 | 211 | 4.4 |
| T3 | 126 | 0 | 0 | 5.61 ± 1.53 | 378 | 5.3 |
| T4 (Case 5) | 300 | 0 | 0 | 6.14 ± 1.53 | 1505 | 6 |
| T5 | 420 | 4 | 20 | 6.41 ± 1.6 | 231 | 6.28 |

employed. In addition to modeling mechanical vibration effects on Pt particle size, the statistical model aimed to predict an average particle size for possibly unobserved vibration conditions (in the range of 0–40 Hz and 0–4 g) and time length (up to 300 h). The effect of time was modeled using a generalized linear model [43] with a hyperbolic tangent link function. This is a consequence of the fact that as time progresses its effect on Pt particle size tends to decrease. The effect of vibration parameters such as frequency (Hz), acceleration (g), and time (t) on particle size was described by a second-degree generalized linear model [44]. The aforementioned considerations lead to the developed statistical model of Eq. (4).

$$\begin{aligned} D_{[i,v]} &= \beta_{off} + \tanh\left(\lambda X_{[i,t]}\right)\left[\beta_t + \beta_{g,t}X_{[i,g]} + \beta_{hz,t}X_{[i,hz]}\right] \\ &\quad + X^2_{[i,hz]}\beta_{hz,hz} + \varepsilon_{i,v} \quad i = n\ldots n_v \\ X_{[:,g]} &= \begin{pmatrix} g_1 \\ \ldots \\ g_{np} \end{pmatrix}; X_{[:,hz]} = \begin{pmatrix} hz_1 \\ \ldots \\ hz_{np} \end{pmatrix}; X_{[:,t]} = \begin{pmatrix} t_1 \\ \ldots \\ t_{np} \end{pmatrix}; \\ \beta &= \left(\beta_{off}, \beta_{g,t}, \beta_t, \beta_{hz,t}, \beta_{hz,hz}\right) \end{aligned} \tag{4}$$

where $X_{[i,t]}$ is the time elapsed; $X_{[i,g]}$ is the acceleration exposure; and $X_{[i,hz]}$ is the frequency applied to the ith particle. $D_{[i,v]}$ is the diameter of ith Pt particle under certain mechanical vibration condition $v$. $\varepsilon_{i,v}$ is the Gaussian residual error. $\beta_{off}$ is the offset parameter (initial Pt particle size at time 0 under 0 g and 0 Hz), $\beta_t$ is the time effect on Pt particle size, $\beta_{g,t}$ is the interaction effect of acceleration and time on Pt particle size, $\beta_{hz,t}$ is the interaction effect of frequency and time on Pt particle size, and $\lambda$ is the parameter governing the Pt particle size growth speed reduction with time. The number of Pt particles observed under mechanical vibration condition $v$ is denoted by $n_v$. $g_1,\ldots,g_{ns}$ is the observed acceleration settings; $hz_1,\ldots,hz_{ns}$ is the observed frequency settings, and $t_1,\ldots,t_{ns}$ is the observed time settings.

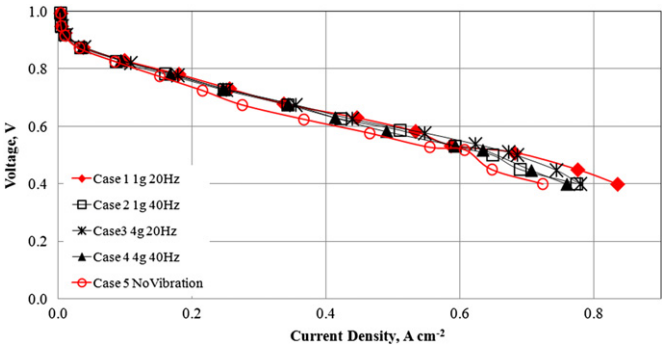


**Fig. 2.** VI curves after 300 h accelerated tests.

## 4. Results and discussion

Fig. 2 shows the performance of the MEA after each of the 300-h accelerated test. It can be seen that after the 300-h accelerated test, the performance of the MEA tested at no vibration conditions (Case 5) degraded the most. The MEA tested at 1 g 20 Hz vibration condition (Case 1) had the best performance compared to other cases. During each of the 300-h accelerated test all parameters, such as temperature, humidity, gases flow rate, pressure, were kept constant and the only variable parameters were frequency (Hz) and acceleration (g). The drop in the performance presumably happened due to the difference in the size of the grown Pt particle ~6 nm (Case 5) and ~5.47 nm (Case 1).

Fig. 3(b–f) shows the TEM images of the cathode side of the MEAs after accelerated tests under various mechanical vibration conditions (Case 1–Case 5). Fig. 4(b–f) shows the TEM images of the cathode side after the various time duration accelerated tests (T1–T5).

Figs. 3 and 4 show an increase in the Pt particle size as well as decrease in the catalyst active area. Fig. 3a shows the TEM image of the cathode in a pristine state. To determine initial Pt particle diameter size five pristine MEAs were analyzed. Initially, Pt loading and particle size on the anode and cathode sides were approximately the same. Analysis of the TEM images of the anode and cathodes sides of the PEMFCs showed that the Pt particle growth on the anode side is minimal and can be neglected. The same observation was noted by Borup et al. [39]. This happens due to high potential on the cathode side ($E^\circ$=1.229 V at cathode under standard conditions, the potential on the anode side is close to 0) and the presence of the water.

For each image the Pt particle total areas and local coordinates were recorded. The diameters were calculated by assuming the shape of Pt particles to be circle [15]. From the obtained TEM images we can see darker spots that are interpreted as the Pt particles. Platinum particle diameter sizes obtained by the TEM for the pristine state and after each accelerated test are presented in Tables 4 and 5. The TEM data is consistent in that the vibrations caused relatively smaller Pt particles.

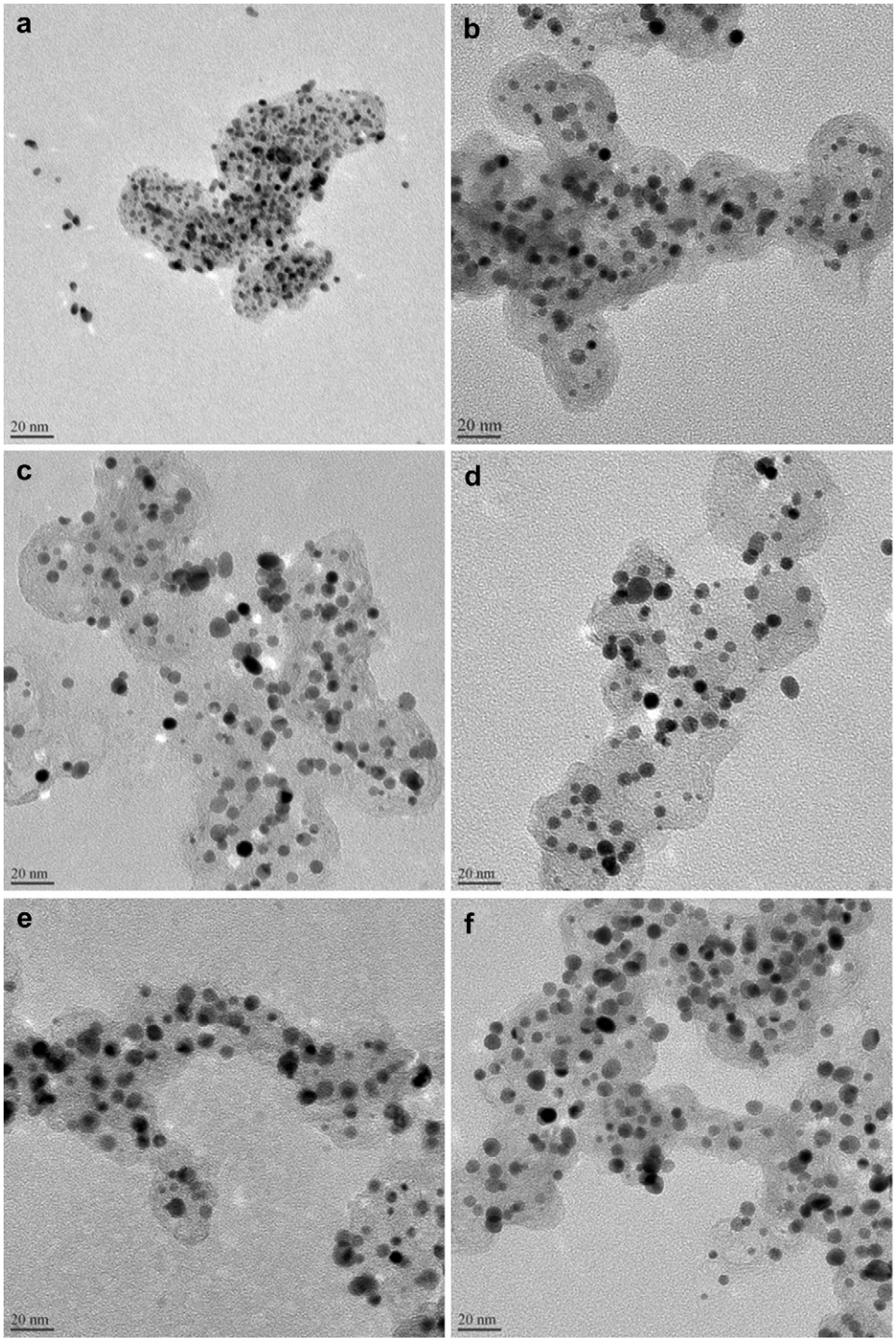


**Fig. 3.** Carbon-supported Pt catalyst layer. TEM Image cathode side. (a) Pristine membrane; (b) Case 1 (1 g 20 Hz); (c) Case 2 (1 g 40 Hz); (d) Case 3 (4 g 20 Hz); (e) Case 4 (4 g 40 Hz); (f) Case 5 (no vibration).

Fig. 5 presents box plots of the Pt particle size distribution on the catalyst layer of pristine and tested MEAs after 300-h accelerated test (Case 1—Case 5). Comparing the box plots for the MEA after the accelerated test, we can say that the Pt particle size distributions in the Case 1, Case 3 and Case 4, are skewed to the right which tells us that significant numbers of Pt particles are above the median size (more particles are in higher size range). The particle size distributions for the Case 2 and Case 5 are close to normal (the number of large and small Pt particles are equal).

The median values for Pt particle diameter sizes after each accelerated test are presented in Tables 4 and 5. Unlike the mean, the median is not influenced by outliers at the extremes of the data set. For this reason, the median is used when there are a few

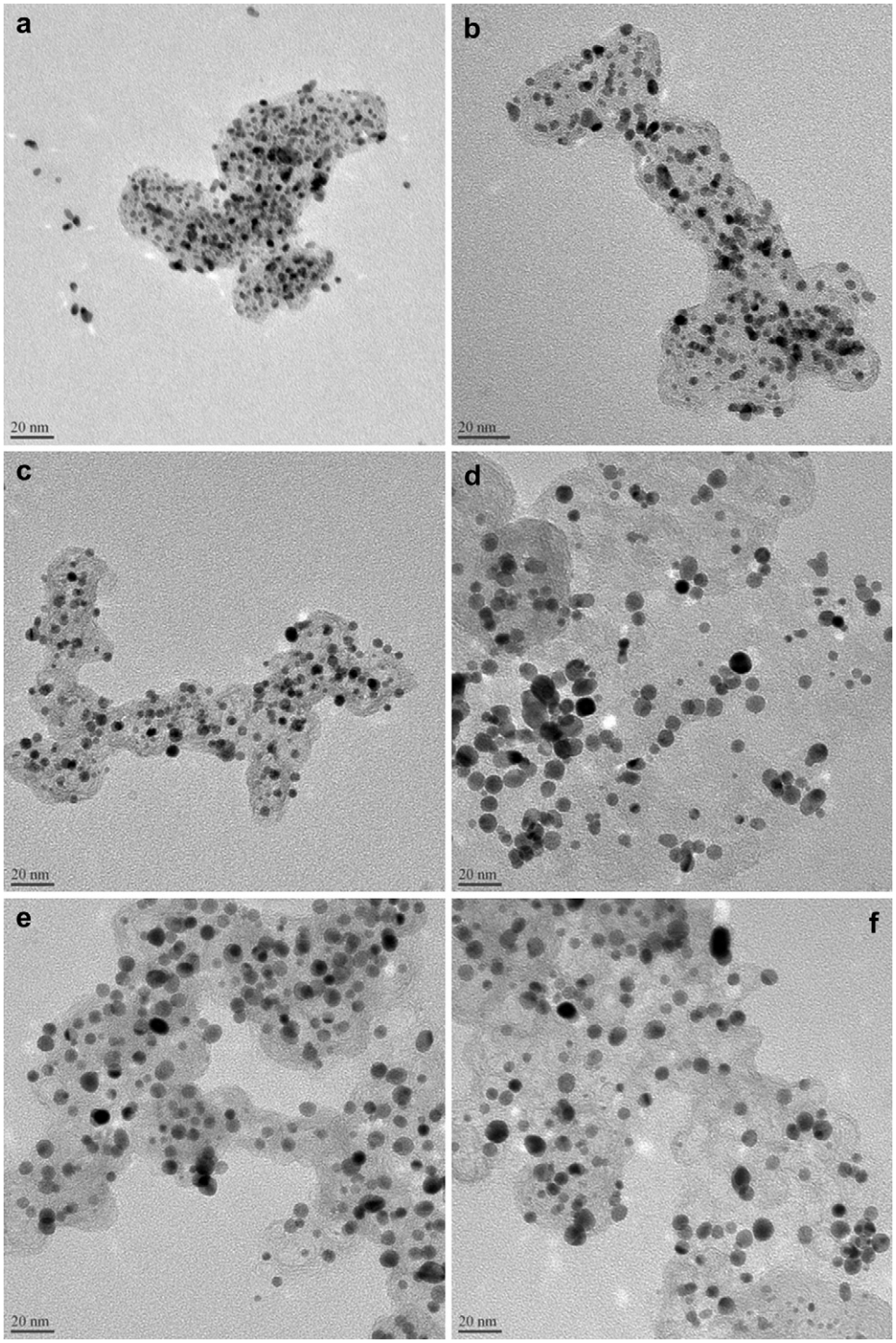


**Fig. 4.** Carbon-supported Pt catalyst layer. TEM Image cathode side. (a) Pristine membrane; (b) T1 (2 h); (c) T2 (50 h); (d) T3 (126 h); (e) T4 (Case 5) (300 h); (f) T5 (420 h).

extreme values that could greatly influence the mean and distort what might be considered typical.

The statistical analyses, including the creation of box plots and running ANOVA and multiple comparison tests, were conducted using MATLAB software [45]. From the ANOVA test, the $p$-value ($p = 2 \cdot 10^{-28}$) suggests that Pt particle mean sizes after 300-h accelerated test under various vibration conditions are significantly different. Therefore, the previously stated null hypothesis, that is, mean Pt particle sizes between each 300-h accelerated test under vibration conditions (Case 1–Case 5) are the same, cannot be accepted.

The results of multiple comparison analysis are presented in a form of matrix and are shown in Table 6. First two columns represent groups for comparison, fourth column shows the difference in means of the groups compared. Third and fifth column are showing a 95% confidence interval for the true difference of the

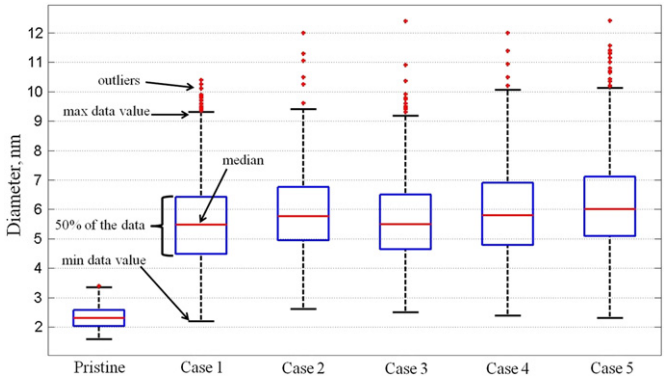


**Fig. 5.** Box plots for Pt particle size distribution after 300-h accelerated test.

means. If the confidence interval does not contain zero value, the difference is significant at the 0.05 level. If the confidence interval contains zero value, the difference is not significant at the 0.05 level. The groups that were not found to be significantly different are highlighted in Table 6 using bold font.

The statistics can also be further explained in Fig. 6. Mean values are represented by circle symbols. Confidence intervals are shown by lines crossing the circle symbols. Two means are significantly different if their intervals are disjoint, and are not significantly different if their intervals overlap. The multiple comparison analysis showed that Pt particle size means after 300-h accelerated test under various mechanical vibration conditions (Cases 1–4) were significantly different from Pt particle sizes tested at no vibration conditions (Case 5). Analysis also revealed significant difference between Pt particle size means tested at 1 g 20 Hz, 4g 20 Hz and 1 g 40 Hz, 4 g 40 Hz, meaning that Case 1 and Case 3 were significantly different from Case 2 and Case 4 mechanical vibration conditions with 95% confidence.

Fig. 7 illustrates predicted and experimentally observed Pt particle diameter size as a function of time under vibration conditions. Fig. 8 shows predicted and experimentally observed Pt particle sizes as a function of frequency under 1 g and 4 g acceleration at fixed time value, i.e., 300-h.

In Fig. 7, it can be shown that there is a fast increase in average Pt particle size between 0 and 50 h but this increase is progressively smaller after about 50 h. In Figs. 7 and 8, it can also be explained that the time and frequency parameters greatly significantly influence the growth of Pt particles. It was also observed that the effect of acceleration is minimal. In Fig. 8, it was observed that the average Pt particle size decreased due to increase in frequency for the values up to 28 Hz but the size for frequencies between 28 and 40 Hz was observed.

We conjectured that the reason for the decrease in Pt particle agglomeration and growth subjected to vibration was due to the hydrogen crossover that reduces the amount of Pt ions on the cathode side. We also observed that mechanical vibrations may

**Table 6**
Case 1–Case 5 multiple comparison matrix.

| Group of comparison | | Lower confidence interval | Mean difference | Upper confidence Interval |
|---|---|---|---|---|
| Case 1 | Case 2 | −0.5275 | −0.3341 | −0.1407 |
| **Case 1** | **Case 3** | **−0.2484** | **−0.0862** | **0.0761** |
| Case 1 | Case 4 | −0.5117 | −0.3372 | −0.1627 |
| Case 1 | Case 5 | −0.7429 | −0.5921 | −0.4414 |
| Case 2 | Case 3 | 0.0486 | 0.2479 | 0.4473 |
| **Case 2** | **Case 4** | **−0.2125** | **−0.0031** | **0.2063** |
| Case 2 | Case 5 | −0.4482 | −0.2580 | −0.0679 |
| Case 3 | Case 4 | −0.4321 | −0.2510 | −0.0700 |
| Case 3 | Case 5 | −0.6643 | −0.5060 | −0.3476 |
| Case 4 | Case 5 | −0.4258 | −0.2549 | −0.0841 |

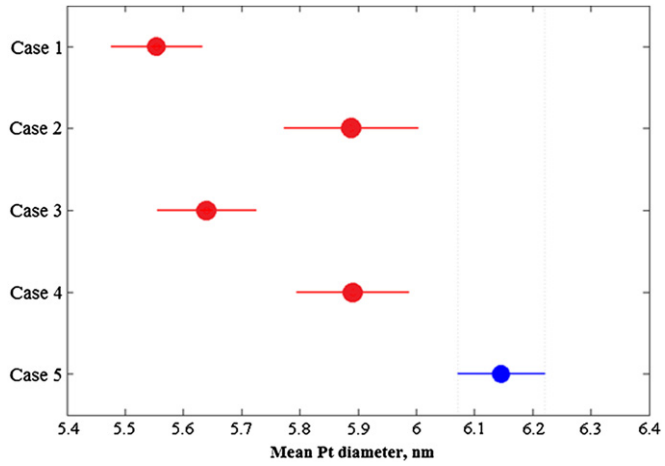


**Fig. 6.** Multiple comparison analysis plot.

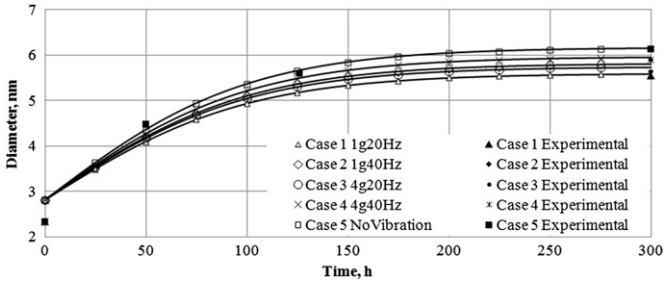


**Fig. 7.** Time (h) versus Pt particle diameter size (nm).

cause the thinning of the MEA, which lead to hydrogen crossover increase. After the accelerated test, we observed degradations of PEMFC components however further studies need to be performed to confirm these observations and link the component degradations to the growth and agglomeration of Pt particles.

From our study, it was evident that the exposure of PEMFC to mechanical vibration in 300 h affects the structural integrity of the cell components, especially the bipolar plates (BP), the gas diffusion layer (GDL), and the MEA. It was observed that there was a loss of compression due to vibrations from the initial compression at a bolt torque value of 13 Nm. Due to the loss of compression, the GDL and the MEA experienced to mechanical shearing stresses that could cause the thinning of the MEA and the increase of GDL porosity. The thinning of the MEA could cause the increase in hydrogen crossover and in short term decrease the rate of Pt agglomeration and growth

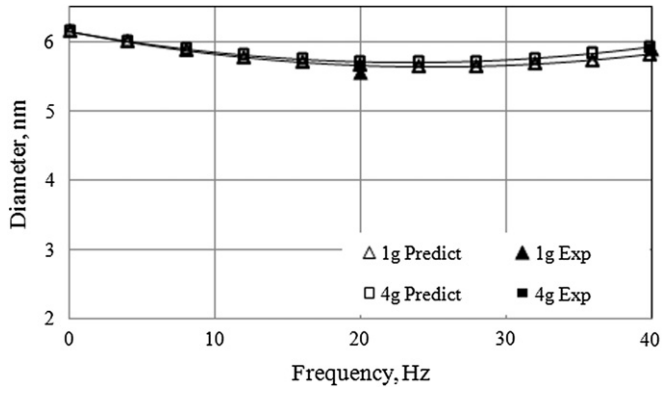


**Fig. 8.** Frequency versus Pt particle average diameter size (nm) under 1 g and 4 g at 300 h.

[17,23–26]. Subjecting PEMFC to vibrations for a longer term will lead to further thinning of the MEA and its permanent damage.

In explaining our observations, we conducted a literature survey on the effect of various chemical and mechanical conditions on the PEMFC performance. The effect of hydrogen crossover, humidity, temperature, and potential conditions on PEMFC performance has been described by many researchers [17–32]. There are also many research groups that studied physicochemical properties and their effect on fuel cell performance and contact resistance [46–53].

For example, Zhou and Wu [46] studied the effect of compression deformation of the GDL on the performance of the PEM fuel cell. A finite element model was developed to analyze the ohmic contact resistance between BP and GDL, the GDL deformation and porosity distribution. When PEMFC components are compressed there several interfacial contacts are to be considered, such as BP/GDL, GDL/catalyst and catalyst/membrane interfaces. Due to elastic deformation the GDL and MEA surfaces go into the BP channel (GDL by about 0.0552 mm–0.1115 mm).

Lee et al. [47] showed that increase in the GDL porosity leads to increase in oxygen consumption, thus higher current densities and better performance. However it may lead to rapid flooding conditions and sharp performance decrease in long term. Mirsha et al. [48,49] studied different gas diffusion layer materials and contact pressure on the electrical contact resistance. A major source of the contact resistances in a fuel cell stack comes from the interface between the GDL and the BP. The clamping of a stack causes a pressure to be applied at the interface, leading to an increase in the contact area between fuel cell components, which in turn decrease the contact resistance. However, a large pressure may deform the gas diffusion layers and membrane, causing cell leakage and internal short. Thus, an optimum clamping pressure exists that trades off between the competing requirements.

We are currently working on investigating the effect of vibration on the long-term degradation of PEMFC components and its effect on PEMFC performance and to relate the degradations to the Pt agglomeration and growth.

## 5. Conclusion

The effect of mechanical vibrations on Pt agglomeration and growth has been investigated using the designed accelerated test and a TEM technique. The microscopy data shows that the Pt particle diameter size is generally smaller under mechanical vibration conditions (Case 1–Case 4). The analysis of TEM images shows that after 300 h accelerated test the average Pt particle size under vibration conditions is 10% smaller than under no vibration condition. The Pt particles on the order of 2–2.5 nm in pristine stated have grown to ~6 nm (no vibration) and ~5.47 nm (1 g 20 Hz). However, among three parameters: time, frequency and acceleration, time is a dominant factor in Pt particles agglomeration and growth.

The statistical multiple comparison showed that Pt particle mean sizes of the catalyst layer tested under 1 g 20 Hz (Case 1) and 4 g 20 Hz (Case 3) mechanical vibration conditions are significantly different, with 95% confidence level, from the Pt particle mean sizes of the catalyst layers tested at different mechanical vibration conditions (Cases 2 and 4). Also Pt particle sizes after 300-h accelerated test at the various mechanical vibration conditions (Case 1–Case 4) are significantly different from the particle sizes after no vibration test (Case 5).

The statistical regression model as well as experimental data showed that particle diameter sizes tend to decrease (as a function of frequency) when frequencies are below 28 Hz and tend to increase for frequency between 28 and 40 Hz. It was also observed that the increase in average diameter size slows significantly after about 50 h of the Fuel Cell operation.

We conjectured that mechanical vibrations caused shearing stresses between the BP, GDL and MEA, which may lead to the thinning of MEA and the increase in hydrogen crossover rate. The hydrogen crossover reduced the amount of Pt ions on the cathode side and decreased the rate of the Pt particle agglomeration and growth. Finally, the influence of mechanical vibrations on the degradation of PEMFC components is currently being studied.

## Acknowledgments

Authors greatly thank Dr. Hongwen Zhou and Dr. Michael Zdilla, both in the Department of Chemistry, Temple University, for their help with TEM imaging and XRD analysis. The authors would also like to thank the US National Science Foundation (EEC 1042071) and the Pennsylvania Department of Environmental Protection Alternative Fuels Incentive Program (AFIG) for the financial support.

## References

[1] J. Mason, Energy Policy 35 (2007) 1315–1329.
[2] T.E. Springer, T.A. Zawodzinski, S. Gottesfeld, Journal of The Electrochemical Society 138 (1991) 2334–2342.
[3] A. Biyikoglu, International Journal of Hydrogen Energy 30 (2005) 1181–1212.
[4] B. Sorensen, Hydrogen and Fuel Cells: Emerging Technologies and Applications, Academic Press, 2005.
[5] Q. Yan, H. Toghiani, H. Causey, Journal of Power Sources 161 (2006) 492–502.
[6] S.Y. Ahn, S.J. Shin, H.Y. Ha, S.A. Hong, Y.C. Lee, T.W. Lim, I.H. Oh, Journal of Power Sources 106 (2002) 500–506.
[7] S.G. Chalk, J.F. Miller, F.W. Wagner, Journal of Power Sources 86 (2000) 40–51.
[8] S. Kundu, M. Cimenti, S. Lee, D. Bessarabov, Membrane Technology 10 (2009) 7–10.
[9] Z. Siroma, K. Ishii, K. Yasuda, M. Inaba, A. Tasaka, Journal of Power Sources 171 (2007) 524–529.
[10] J. Xie, L.D. Wood III, L.K. More, P. Atanassov, R. Borup, Journal of The Electrochemical Society 152 (5) (2005) A1011–A1020.
[11] W. Bi, T.F. Fuller, Journal of Power Sources 178 (2008) 188–196.
[12] S. Zhang, X.Z. Yuana, J.C. Hina, H. Wanga, A. Friedrich, M. Schulze, Journal of Power Sources 19 (2009) 588–600.
[13] G.J.M. Janssen, E.F. Sitters, A. Pfrang, Journal of Power Sources 191 (2009) 501–509.
[14] S. Lee, D. Bessarabov, R. Vohra, In: Proceedings of the Hydrogen and Fuel Cell, International Conference, Vancouver, BC, Canada, 2009.
[15] K.J.J. Mayrhofer, J.C. Meier, S.J. Ashton, G.K.H. Wiberg, F. Kraus, M. Hanzlik, M. Arenz, Electrochemistry Communications 10 (2008) 1144–1147.
[16] F.A. De Bruijn, V.A.T. Dam, G.J.M. Janssen, Fuel Cells 8 (2008) 3.
[17] K. Yasuda, A. Taniguchi, T. Akita, T. Ioroi, Z. Siroma, Physical Chemistry Chemical Physics 8 (2006) 746.
[18] R. Lin, B. Lin, Y.P. Hou, J.M. Ma, International Journal of Hydrogen Energy 34 (2009) 2369–2376.
[19] X. Yu, S. Ye, Journal of Power Sources 172 (2007) 145–154.
[20] H.A. Gasteiger, S.S. Kocha, B. Sompalli, F.T. Wagner, Applied Catalysis B: Environmental 56 (2005) 9–35.
[21] E. Antolini, J.R.C. Salgado, E.R. Gonzalez, Journal of Power Sources 160 (2006) 957–968.
[22] Y. Shao, G. Yin, Y. Gao, Journal of Power Sources 171 (2007) 558–566.
[23] R.M. Darling, J.P. Meyers, Journal of The Electrochemical Society 150 (2003) A1523–A1527.
[24] T.T.H. Chen, E. Rogers, A.P. Young, S. Ye, V. Colbow, S. Wessel, Journal of Power Sources 196 (2011) 7985–7988.
[25] E.F. Holby, W. Sheng, Y. Shao-Horn, D. Morgan, Energy & Environmental Science 2 (2009) 865–871.
[26] P.J. Ferreira, G.J. Ia O', Y. Shao-Horn, D. Morgan, R. Makharia, S. Kocha, H.A. Gasteiger, Journal of The Electrochemical Society 12 (11) (2005) 2256–2271.
[27] G. Diloyan, L. Breziner, P. Hutapea, ASME Journal of Fuel Cell Science and Technology 9 (2012) 034502, 1–6.
[28] P. Strahs, J. Weaver, L.C. Breziner, C. Garant, K. Shaffer, G. Diloyan, P. Hutapea, Journal of Renewable and Sustainable Energy 3 (2012).
[29] N. Rajalakshmi, S. Pandian, K.S. Dhathatheryan, International Journal of Hydrogen Energy 34 (2009) 3833–3837.
[30] V. Rouss, W. Charon, Journal of Power Sources 175 (2008) 1–17.
[31] M.C. Bétournay, G. Bonnell, E. Edwardson, D. Paktunc, A. Kaufman, A.T. Lomma, Journal of Power Sources 134 (2004) 80–87.
[32] Z. Luo, D. Li, H. Tang, M. Pan, R. Ruan, International Journal of Hydrogen Energy 31 (2006) 1831–1837.
[33] K.L. More, R. Borup, K.S. Reeves, ECS Transitions 3 (2006) 717–733.
[34] N.L. Garland, T.G. Benjamin, J.P. Kopasz, ECS Transitions 11 (2007) 923–931.
[35] S. Mitsushima, S. Kawahara, K. Ota, N. Kamiya, Journal of The Electrochemical Society 154 (2) (2007) B153–B158.
[36] P. Pei, X. Yuan, P. Chao, X. Wang, International Journal of Hydrogen Energy 35 (7) (2009) 1–5.

[37] US Fuel Cell Councils, Protocol on Fuel Cell Component Testing, USFCC04–003 (2004).
[38] DOE Cell Component Accelerated Stress Test Protocols for PEM Fuel Cells (Electrocatalysts, Supports, Membranes, and Membrane Electrode Assemblies), http://www1.eere.energy.gov/hydrogenandfuelcells/fuelcells/pdfs/component_durability_profile.pdf.
[39] R.L. Borup, J.R. Davey, F.H. Garzon, D.L. Wood, Journal of Power Sources 163 (2006) 76–81.
[40] S. Yildirim, S. Erkaya, I. Eski, I. Uzmay, Journal of Vibration and Control 15 (2009) 133–156.
[41] National Institute of Health, ImageJ, Image Processing and Analysis in Java, http://rsbweb.nih.gov/ij/.
[42] D.C. Montgomery, G.C. Runger, Applied Statistics and Probability for Engineers, John Wiley and Sons, 2010.
[43] P. McCullagh, J.A. Nelder, Generalized Linear Models, second ed. Chapman and Hall, 1989.
[44] N. Draper, H. Smith, Applied Regression Analysis, second ed. Wiley Series in Probability and Mathematical Statistics, 1981.
[45] MathWorks Inc., Matlab (Matrix Laboratory), http://www.mathworks.com.
[46] P. Zhou, C.W. Wu, Journal of Power Sources 170 (2007) 93–100.
[47] H.K. Lee, J.H. Park, D.Y. Kim, T.H. Lee, Journal of Power Sources 123 (2003) 1–9.
[48] V. Mishra, F. Yang, R. Pitchumani, Transitions of the ASME 1 (2004) 1–8.
[49] V. Mishra, F. Yang, R. Pitchumani, 141 (2005) 47–64.
[50] J. Ihonen, F. Jaouen, G. Lindbergh, G. Sundholm, Electrochimica Acta 46 (2001) 2899–2911.
[51] W.R. Chang, J.J. Hwang, F.B. Weng, S.H. Chan, Journal of Power Sources 166 (2007) 149–154.
[52] J. Ge, A. Higer, H. Liu, Journal of Power Sources 159 (2006) 922–927.
[53] L. Xianguo, S. Imran, International Journal of Hydrogen Energy 30 (2005) 359–371.

## Nomenclature

$X_{[i,t]}$: time elapsed
$X_{[i,g]}$: acceleration exposure to ith Pt particle
$X_{[i,hz]}$: frequency applied to ith Pt particle
$D$: diameter of ith Pt particle under certain mechanical vibration condition '$v$'
$\varepsilon$: Gaussian residual error
$\beta$: the offset parameter (initial Pt particle size at time 0 under 0 g and 0 Hz)
$\beta$: the time effect on Pt particle size
$\beta_{g,t}$: the interaction effect of acceleration and time on Pt particle size
$\beta_{hz,t}$: the interaction effect of frequency and time on Pt particle size
$\lambda$: the parameter governing how fast the effects of time reducing the speed of Pt particle size growth
$g_1,\ldots,g_{ns}$: acceleration settings observed
$hz_1,\ldots,hz_{ns}$: frequency settings observed
$t_1,\ldots,t_{ns}$: time settings observed